

T.Kasuga, H.Yonehara, M.Hasumoto, and T.Kinoshita
 Institute for Molecular Science
 Myodaiji-cho, Okazaki, 444 Japan

Abstract

UVSOR is a 600 MeV electron storage ring dedicated to ultraviolet synchrotron orbital radiation research in molecular science and related fields. Measurements of horizontal and vertical orbit distortions are important to detect displacements of radiant points of synchrotron radiation and to correct the orbit distortions. Sixteen position monitors are installed in the ring, and each position monitor consists of four button type electrodes. One of sixty four electrodes is selected by a coaxial switch multiplexer system, and signal from the electrode is detected by a linear detector. Data from the detector are taken by a micro-computer system and orbit distortion is calculated by the computer. An orbit distortion is corrected by means of eight vertical steering magnets and eight trim coils wound on bending magnets. Optimum excitation currents for the steering magnets and the trim coils to correct the orbit distortions are calculated by the computer. Reductions of horizontal and vertical orbit distortions are a half and a third respectively.

Design of Electrode Configuration

As a cross-section of a doughnut of a bending section of the storage ring is rectangular, an electric field induced by electron beam in the doughnut can be calculated by an analytic method. As the electron velocity is very close to the velocity of light, the electric field in the doughnut is calculated from the solution of two-dimensional Poisson equation,

$$\nabla^2\phi = -D_\lambda\delta(x-x_0)\delta(y-y_0)/\epsilon_0 \quad (1)$$

where ϕ the potential at (x,y) , ϵ_0 the permibility of free space, (x_0,y_0) the coordinate of the beam and D_λ is the line charge density of the beam.

We work in rectangular coordinate (Fig. 1). A solution of eq (1) is,

$$\phi = \begin{cases} D_\lambda \sum_{m=1}^{\infty} \frac{\sinh a_m(b-y_0) \sinh a_m(y+b)}{\epsilon_0 a_m \sinh 2ba_m} x & y \leq y_0 \\ D_\lambda \sum_{m=1}^{\infty} \frac{\sinh a_m(b+y_0) \sinh a_m(b-y)}{\epsilon_0 a_m \sinh 2ba_m} x & y > y_0 \end{cases} \quad (2)$$

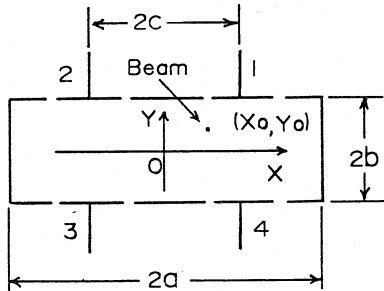


Fig. 1 Coordinate System

where a, b are shown in Fig. 1 and $a_m = m\pi/2a$. y components of the electric field at four electrodes whose coordinates are (c,b) , $(-c,b)$, $(-c,-b)$ and $(c,-b)$ are,

$$\begin{aligned} E_1 &= E_y(c, b) = -\frac{\partial\phi(c, b)}{\partial y} \\ &= D_\lambda \sum \frac{\sinh a_m(y_0+b)}{\epsilon_0 a_m \sinh 2ba_m} \sin \frac{m\pi(x_0+a)}{2a} \sin \frac{m\pi(c+a)}{2a} \\ E_2 &= E_y(-c, b) = -\frac{\partial\phi(-c, b)}{\partial y} \\ &= D_\lambda \sum \frac{\sinh a_m(y_0+b)}{\epsilon_0 a_m \sinh 2ba_m} \sin \frac{m\pi(x_0+a)}{2a} \sin \frac{m\pi(-c+a)}{2a} \\ E_3 &= E_y(-c, -b) = -\frac{\partial\phi(-c, -b)}{\partial y} \\ &= -D_\lambda \sum \frac{\sinh a_m(b-y_0)}{\epsilon_0 a_m \sinh 2ba_m} \sin \frac{m\pi(x_0+a)}{2a} \sin \frac{m\pi(-c+a)}{2a} \\ E_4 &= E_y(c, -b) = -\frac{\partial\phi(c, -b)}{\partial y} \\ &= -D_\lambda \sum \frac{\sinh a_m(b-y_0)}{\epsilon_0 a_m \sinh 2ba_m} \sin \frac{m\pi(x_0+a)}{2a} \sin \frac{m\pi(c+a)}{2a} \end{aligned} \quad (3)$$

As output voltages of four electrodes are proportional to the y components of the electric field, small orbit displacement (x_0, y_0) can be calculated by,

$$\begin{aligned} x_0 &= \eta \frac{V_1 - V_2 - V_3 + V_4}{V_1 + V_2 + V_3 + V_4} \\ y_0 &= \zeta \frac{V_1 + V_2 - V_3 - V_4}{V_1 + V_2 + V_3 + V_4} \end{aligned} \quad (4)$$

where V_i ($i=1, \dots, 4$) are output voltages of the four electrodes, and η and ζ are given by

$$\begin{aligned} \eta &= \frac{\sqrt{2}\pi}{a} \frac{1/\cosh(b\pi/a) - 3/\cosh(3b\pi/a) + 5/\cosh(5b\pi/a) - \dots}{1/\cosh(b\pi/2a) - 1/\cosh(3b\pi/2a) - 1/\cosh(5b\pi/2a) + \dots} \\ \zeta &= \frac{\sqrt{2}\pi a}{b} \frac{\sinh(a\pi/2b)/\cosh(a\pi/b) - 2\sinh(2a\pi/2b)/\cosh(2a\pi/b) + \dots}{1/\cosh(b\pi/2a) - 1/\cosh(3b\pi/2a) - 1/\cosh(5b\pi/2a) + \dots} \end{aligned} \quad (5)$$

In our case, $a=55\text{mm}$, $b=19\text{mm}$ and $c=27.5\text{mm}$ then $\eta=12.3\text{mm}$ and $\zeta=58.9\text{mm}$. Position measurement errors due to sensitivity errors of four electrodes are 1.4 mm (horizontal) and 7mm (vertical) per 1 dB sensitivity error.

The structure of the position monitor is shown in Fig. 2. Each button is mounted on a BNC type feedthrough which is welded on a flange, and it is easily exchangeable. Sixteen monitors are installed on both sides of eight bending magnets.

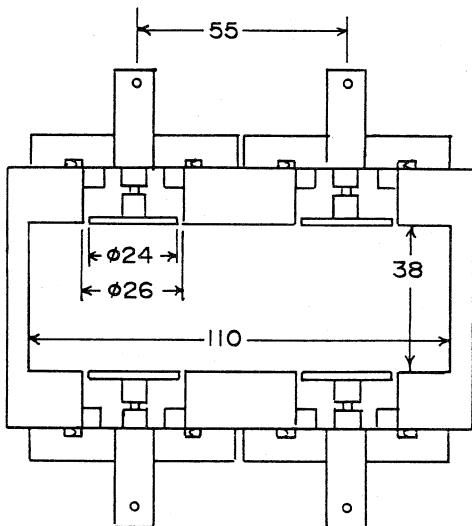


Fig. 2 Structure of Monitor

Bench Test

A model of the monitor was made and the sensitivities were measured. An antenna rod which simulated an electron beam was inserted into the model monitor, and RF signal from a signal generator of 90.12 MHz (radio frequency of the acceleration system) was supplied to it. Output levels of electrodes were measured by a spectrum analyzer which was used as a selective detector of 90.12 MHz.

Measured sensitivities were,

$$\begin{aligned} \eta_{MES} &= 12.5 \quad (\text{mm}) \\ \zeta_{MES} &= 39.8 \quad (\text{mm}) \end{aligned} \quad (6)$$

An agreement between measured horizontal sensitivity and calculated η is quite well, but measured vertical sensitivity is different from calculated ζ . Because the infinitesimal size of electrodes is assumed in the calculation, the disagreement is due to the finite size of electrodes. The problem of size is not severe for the horizontal sensitivity because of the configuration of the four electrodes.

As mentioned before, errors due to the lack of uniformity of four electrodes are not negligible. All sensitivities of sixty four electrodes (4 electrodes/Monitor x 16 Monitors) were measured and stored in a memory of a micro-computer to correct the sensitivity differences. The accuracy of the measurements was better than 0.1 dB, and estimated errors of the beam position measurement due to the sensitivity errors are less than 0.14 mm (horizontal) and 0.7 mm (vertical). As this measurement was done using whole system including the multiplexer system, losses in cables and coaxial switches were corrected at the same time.

Beam Position Detection System

A multiplexer system which consists of fast coaxial switches is shown in Fig. 3. The coaxial switches are controlled by the micro-computer which is settled in the control room.

Output signal selected by the multiplexer system is detected by a 90.12 MHz linear detector in the storage ring room. The linear detector is a superheterodyne type. 90.12 MHz component and an output of a local oscillator whose frequency is 79.42 MHz ($= 90.12 - 10.7$ MHz, 10.7 MHz : intermediate frequency) are mixed, an intermediate frequency is amplified and detected. A master oscillator for the acceleration system is set in the control room. Signals from the master oscillator and from a 10.7 MHz crystal oscillator are mixed, and the frequency of the

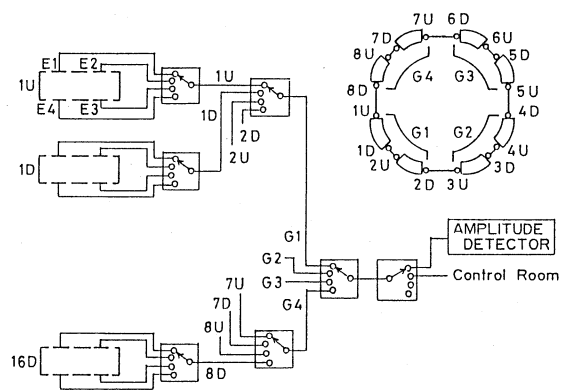


Fig. 3 Multiplexer System

local oscillator is synthesized. Therefore the intermediate frequency is not changed even though the frequency of the master oscillator is changed. The output of the local oscillator is transmitted to the storage ring room and fed to the linear detector. A blockdiagram of the linear detector is shown in Fig. 4. The main part of the linear detector is a fast Schottky diode, and non-linearity of the diode is compensated by a feedback circuit. To ensure wide dynamic range of the linear detector, a programmable attenuator which is controlled from the control room is used. D.C. voltage from the linear detector which is proportional to the level of 90.12 MHz component is transmitted to the control room, and digitized by an AD converter in the computer system. As the sensitivity of the 90.12 MHz linear detector is high, an orbit distortion of low current beam ($\sim 1\text{mA}$, $1/500$ of designed beam current) can be measured.

The sensitivity errors of the sixty four electrodes are corrected, horizontal and vertical beam positions are calculated and printed out by the computer system.

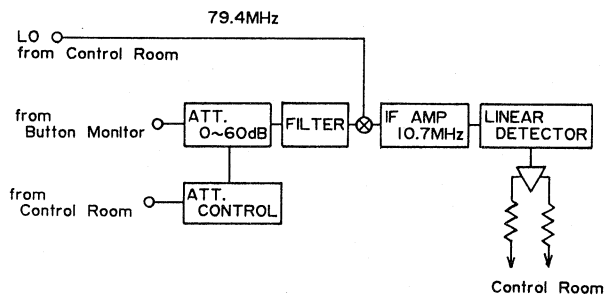


Fig. 4 Blockdiagram of Linear detector

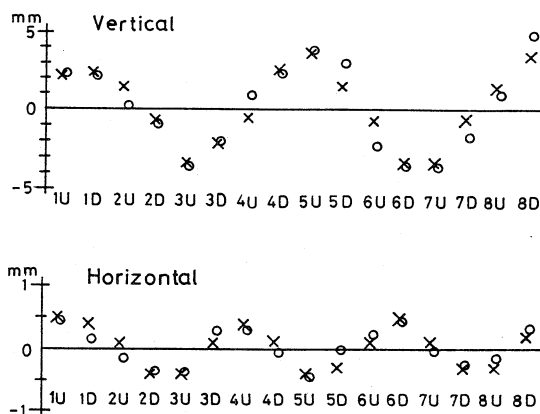


Fig. 5 Orbit Distortion Formed by Correction Element

An example of results of orbit distortion measurement is shown in Fig. 5. Horizontal and vertical closed orbit distortions are formed artificially by exciting a trim coil of a bending magnet or a vertical steering magnet to test the performance of the beam position detection system. Crosses in Fig.5 show estimated orbit distortion and circles show measured orbit distortion which is newly generated by the excitation of the trim coil or the steering magnet, i.e. it is the difference of the artificial closed orbit and the orbit without the excitation.

Correction of Orbit Distortion

Trim coils wound on eight bending magnets and eight vertical steering magnets are available to correct the orbit distortions. Excitation currents of trim coils and steering magnets must be determined. Some methods can be applicable to find a set of the deflection angles to be applied to the correction elements. We used "least squares method" to compensate the orbit distortions. $\vec{x}' = \begin{pmatrix} x'_1 \\ \vdots \\ x'_{16} \end{pmatrix}$ denotes

beam displacement at sixteen position monitor points due to $\vec{b} = \begin{pmatrix} b_1 \\ \vdots \\ b_8 \end{pmatrix}$ which is a set of excitation of the

trim coils or the steering magnets, and $\vec{x}' = M\vec{b}$ where M is a 16x8 matrix. The beam position after correction is,

$$\vec{\Delta} = \vec{x} - \vec{x}' = \vec{x} - M\vec{b} \quad (7)$$

where \vec{x} is a beam position without correction. The condition of b for the least squares method is,

$$\vec{b} = ({}^t M M)^{-1} \cdot {}^t M \vec{x} \quad (8)$$

A computer program which calculated the optimum excitation current b was written. Matrix elements of M were determined by measurements of orbit displacements due to the excitation of the correction magnets. In Fig. 6, circles show closed orbit distortions due to magnet errors or alignment errors without the orbit correction. Maximum horizontal and

vertical excursions are ± 5 mm and ± 3.6 mm respectively. Crosses in Fig. 6 show corrected orbit distortions. Orbit excursions are reduced to ± 2 mm and ± 1 mm respectively. The horizontal aperture is limited at the injection point (the space between the designed orbit and the wall of chamber for the septum magnet is 27.5 mm) and the vertical aperture is limited at the beam pipes for the superconducting wiggler and the undulator (the height of the pipes is 20 mm). The residual orbit distortions are small enough as compared with the apertures.

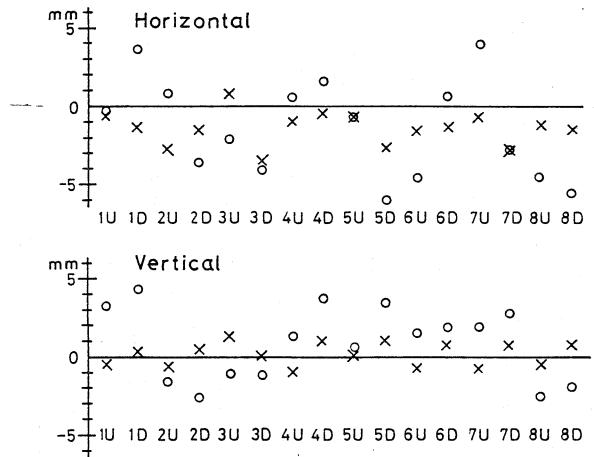


Fig. 6 Results of Orbit Correction

Acknowledgement

We would like to thank T. Katsura and A. Ando of KEK for his suggestions in several discussions, and also our many colleagues in the UVSOR group who contributed to this work.

References

- 1) J. Cuperus, "Monitoring of particle beams at high frequencies", CERN/PS/LIN 76-7 (1976).
- 2) J. D. Jackson, "Classical electrodynamics" (John Wiley & Sons, Inc.) (1975).
- 3) A. Ando and K. Endo, "Correction of closed orbit at injection in alternating-gradient synchrotron", KEK-75-4 (1975).
- 4) B. Autin and P.J. Bryant, "Closed orbit manipulation and correction in the CERN ISR", CERN-ISR-MA/71-36 (1971).